EFFECTS OF TOPOGRAPHIC BLOCKAGE AND OCEAN BOUNDARIES ON LOW FREQUENCY NOISE FIELDS

by

Aubrey Anderson
ONR Detachment, Bay St. Louis, MS
Robert Martin
Samuel Marshall
Naval Ocean Research and Development Activity
NSTL Station, MS

ABSTRACT

Low frequency noise in most ocean areas is dominated by shipping or industrial noise. The composite noise field is the result of radiated energy from each discrete noise source propagating over relatively large distances to the receiving site. The ocean bottom in general, and topographic features in particular, result in vertically directional noise fields in addition to the expected azimuthal directionality. The noise field near the surface displays broadband coherent interaction between the direct and surface image energy, the details of which can be traced in part to the intervening topography. At deeper depths the level versus depth curves also display the impact of the topographic blockage. A measured data set displaying near surface to near bottom low frequency noise levels is analyzed with respect to range dependent environmental factors and shipping densities.

INTRODUCTION

Recently, the depth dependence of the low frequency ocean ambient noise field has been a subject of some interest[1]. Depth profiles of ambient noise were obtained from two AUTOBUOY dives to depths of 2800 m which were conducted at widely separated sites under moderate sea conditions as part of the NORLANT '72 experiment[2]. In both cases no ship traffic was observed in the general area of the dive. The deployment vessel, USNS SANDS (T-AGOR-6), was at quiet ship condition during most of each dive (using only its gas turbine on the 02 level to power the ship's facilities) at a distance of 5 nm from the launch point for the first dive on 22 July and 2 nm from the launchpoint for the second dive on 31 July 1972. Aural and graphical monitoring of the recorded data indicated that no obvious nearby ship noise was present. There were, however, waterborne transients occurring at repetition intervals of approximately 10, 18, and 24 seconds. These transients had low frequency characteristics and time durations which indicate that their sources were some distance away and these have been identified as sparkers and air-guns being used for sub-bottom profiling in the Labrador Basin and over the Grand Banks. The effect of these impulses

on the ambient level was eliminated by processing only in the interval between pulses. Thus, the data reported here represent only ambient noise generated by the sea surface and distant shipping.

The resulting data display different noise level versus depth relationships at the two sites. Furthermore, at one site data were acquired to very shallow depths and near-surface interference was observed in the resulting noise versus depth patterns. Two noise models, DANES[3] and FANM[4], were tested against the data to determine their utility in describing the observations. In addition, the range dependent Parabolic Equation[5] transmission loss model was used to assess the effects of seafloor bathymetry on noise versus depth resulting from distant shipping.

AUTOBUOY DESCRIPTION

AUTOBUOY[6] is a self-contained, untethered, programmable, free-diving, acoustic data gathering system which is capable of maximum depths to 6,000 m. It is generally programmed to descend quickly to a selected maximum depth, to release a descent weight in order to achieve neutral buoyancy and then to hover sequentially at four shallower depths. At each depth, several types of data are recorded on the seven channel tape recorder located in the instrumentation pressure vessel. These data include calibration signals and the acoustic signals from each of two closely spaced ($\sim$10 m) hydrophones together with depth, time, ascent velocity and temperature signals. Depth is controlled during the dive by adjusting the buoyancy around a neutral value in response to depth and velocity error signals. This is accomplished by the alternate valving to sea of light and heavy fluids. While hovering, AUTOBUOY is free to move with the water mass. Thus, no local noise is generated by water flow past the hydrophones. The fluid valving system is operated by solenoids which open valves such that fluid flows out by gravitational force. No noise is detectable from this operation. The depth and velocity signals also determine start times of an analog tape recorder which is preprogrammed for a specific sample size (typically 20 minutes). When recording is completed, the tape is stopped and AUTOBUOY ascends to the next programmed depth. When the last depth station is completed, the system rises to the surface where an attached recovery system, consisting of an rf beacon and a flashing light, is activated.

DIVE DESCRIPTIONS

The dive sites for NORLANT '72[2] are shown in Figure 1. Dive 1 occurred in the northeastern section of the Labrador Sea between Greenland and the Reykjanes Ridge. Dive 2 occurred in the deeper area of the basin 350 nm due south of the southern tip of Greenland. For each dive, AUTOBUOY was programmed to descend to 2900 m and then to hover at 2300, 1700, 1200 and 600 m depths while recording 20 minutes of ambient noise at each depth. At

the shallowest depth station, recording continued until the tape ran out. Figures 2a and 3a pictorially display the actual dive patterns for each event. During the first dive, hovering was achieved only at the two deepest depths while during the second dive hovering occurred at all but the shallowest depth. When hovering did not occur, ascent rates were approximately 1.2 m/sec (about 0.25 kt). At this slow speed, no observable mechanical or flow noise is introduced into the hydrophones. Failure to hover during a depth station is usually the result of valving too much heavy fluid at the deeper depths and not having sufficient reserve for the shallower depths. Also indicated on Figures 2a and 3a are the ship and wind speed conditions during the dives.

SPECTRAL ESTIMATES AND DEPTH DEPENDENT RESULTS

Figures 2b and 3b show the resulting spectra from the hydrophone acoustic outputs for the two dives. Two hydrophones, vertically separated by ~10 m, yielded virtually identical results. All data were processed in 1/3-octave bands centered at the indicated frequencies. Data were processed twice: once on board the SANDS through log-amplifiers onto a strip chart recorder and later ashore using a digital automatic data processing system (ADP). In both cases all transients (seismics, airguns, etc.,) were eliminated from the data. Calibration signals over the entire band were injected at the hydrophone preamplifiers in the laboratory prior to deployment to produce a calibration tape. Also, a broadband calibration signal was automatically injected at the recorder inputs during the dive at the start of each 20 minute segment. The shipboard and ADP results were essentially identical. The principal difference between the spectra for the two dives is their depth dependence. At the deepest depth, the spectrum of the 22 July data has a variation in level with frequency of only 7 dB over the range 25 Hz to 800 Hz. As depth decreases the spectra slowly approach a more familiar shape. The leveling off of the spectra between 200-1000 Hz is a characteristic noted by others[7,8] and is attributed to the overlap between ship generated noise and wind generated noise. In order for this to be the explanation of the 22 July spectra depth dependence, a significant reduction in ship noise contribution would be required for the deep data.

Figures 2c and 3c show the same data plotted to display the noise depth dependence at the two sites. Each data set represents measurements over approximately 6 hours with depths measured sequentially, rather than concurrently. Nevertheless, in the absence of individual nearby noise sources, the data should be a valid representation of persistent background noise as a function of depth for the measured locations and for the conditions that exist in the summer months. Horizontal noise pattern measurements in the northeast Pacific by R. Wagstaff[9], for instance, demonstrate repeatable results from year to year for the same season in the shipping noise dominated portion of the spectrum.

Several interesting features of the noise depth dependence can be noted from the data displayed in Figures 2 and 3. The most striking is the strong depth dependence of the low frequency noise below critical depth

(see the sound speed profile on Figure 2c) at the location of Dive 1. This low frequency noise reduction below critical depth is consistent with observations in other ocean basins[1]. It results in part because most of the energy from the distant noise sources is carried by low order normal modes of the water column and for these modes the amplitude decays exponentially with depth below the critical depth. The rate of decay of the noise level with depth below critical is determined by the energy distribution among the normal modes. This distribution is governed by several factors including: the distribution of energy among the normal modes of the water column of the source region(s), changes in the distribution of noise energy among modes as the energy travels from sources to receiver through a water column with horizontally changing sound speed versus depth structure (and thus changing normal mode eigenfunctions); varying modal attenuation along the propagation path resulting from several factors including bottom interaction of the modes. We will return to a discussion of some of these factors below when comparisons are made with numerical model noise computations.

Other notable features of the noise depth profiles include the virtually constant level with depth for frequencies above 300 Hz at the site of Dive 1 (Figure 2c) and the much weaker depth dependence throughout the water column at the site of Dive 2 for all frequencies as compared with the low frequencies at the site of Dive 1.

DEPTH DEPENDENCE ANALYSIS

Two computerized ambient noise numerical models were used to produce simulations of the noise fields for the sites of Dives 1 and 2. The models used are DANES[3] and FANM[4]. Transmission loss models are useful for analyzing some features of the noise field depth dependence. For this purpose, simulations were run using the Parabolic Equation (PE) computer numerical transmission loss model of Tappert[5]. In this section, the models and model inputs are briefly described. Subsequently, model simulations are compared with the NORLANT '72 AUTOBUOY data and the comparisons are discussed.

The FANM ambient noise model is essentially a computer implementation of the Talham model[10]. It treats water column parameters as range independent (single sound speed profile), but allows bottom depth and bottom loss to vary with range; thus, energy from distant ships can be cut off by intervening bathymetric features. DANES utilizes a fully range dependent environment with propagation described by a range averaged transmission loss for 15^{o} resolution tracks. Data bases for sound velocity profiles (by season and area), bottom loss provinces, bottom depths and shipping distribution (by month) are accessed by DANES as indicated by input information (site location, time of year, weather). Sources are characterized as a function of frequency, by a source at depth of 6 m; source spectra are modified ROSS-ALVAREZ and ship distribution was obtained from the RMS data base. Similar data bases for bottom depth, bottom loss and shipping distribution were accessed by FANM. Figure 4 summarizes the ship count data base. This data base contains ship counts in 1^{o} by 1^{o}

(Lat./Long.) squares. The data are shown in Figure 4 using revised divisions which more clearly indicate the relationship of ship counts, the bottom bathymetry and the measurement sites. Aerial reconnaissance during NORLANT '72[2] identified only 5 ships in a 5^{o} square area near the measurement sites. No ships were observed from the SANDS during the measurements at the site of Dive 1. The higher density shipping to the south in the region shown in Figure 4 is expected because of shipping lanes in this area.

In Figure 5, the NORLANT data at 25 Hz and 50 Hz are compared with the simulated ambient noise depth profile from the DANES model. DANES was executed with a sound speed profile for the Dive 2 site which was measured during NORLANT '72 and with archival sound speed profiles in other portions of the area. Other data bases needed (ship distribution, bottom type, etc.), were accessed as appropriate to the model. Although the DANES simulated noise levels are reasonably close to the measurements at shallow depths, the details of the depth dependence differ between data and model. FANM simulated results (with similar input parameters) at 25 Hz are also shown on Figure 5. They agree with the data less than the DANES results at shallow depths and exhibit a greater change in level with depth than either the data or the DANES simulations. It has been shown[11] that range averaged transmission loss simulations can be valuable in analyzing the depth dependence of ambient noise fields. Such simulations were made using a Parabolic Equation[5] computer model with a noise source depth assumed to be 6 m and with range varying input parameters for bottom bathymetry and sound speed profiles as shown in Fig 6b. These input parameters are representative of the environment to the south of the Dive 2 site, in the direction of most of the noise sources (ships). Results of these transmission loss simulations, averaged over a source-to-receiver range interval of 500 to 600 nm are also shown in Figure 5. The simulations shown are from a low loss bottom (0.2 dB/nm sediment attenuation). It is significant that, while they differ in terms of the details of the noise level versus depth profile, in general, all of the simulation results agree with the data in describing only a small (at most) dependence of noise level on depth over the sampled depth interval.

A more interesting set of comparisons is shown in Figure 7, wherein NORLANT results for the Dive 1 site are shown in comparison with DANES noise and PE average transmission loss depth profiles at 25 Hz and 50 Hz and with FANM noise depth profiles at 25 Hz. There is clearly significant disagreement between the measurements and all of the simulations. The monotonic decrease of measured noise levels with depth is significantly greater than either noise model simulation and the character of the average transmission loss profile disagrees with the measurements especially in the sharp increase in loss (which would produce a similar decrease in noise level) below about 2000 m. This situation has been analyzed further by a parametric study of the inpact of: a) the range dependent nature (horizontal variation) of the sound speed profile in this area; and b) the topographic blockage introduced by the Reykjanes Ridge which is between the receiving site for Dive 1 and most of the ship noise sources (Figure 4). A Parabolic Equation model was used in this study; the basic assumption is that the major contributor to the noise field at the Dive 1 site is distant shipping as local shipping was non-existent. The majority of the distant shipping lies on the far side of the Reykjanes Ridge at distances greater than 300 nm. The Ridge is of varying depth, having a somewhat average

monotonic decline from the surface at Iceland in the northeast to the Labrador Basin in the southwest, ending approximately due south of the southern tip of Greenland. The PE model runs used a source at 6 m depth and were made to a range of 600 nm from the receiver. The water depth at the source was chosen as 4500 m rising to 3300 m at the start of the Reykjanes Ridge, which was chosen as the midway point. The base of the Ridge was assumed to be 200 nm wide with the Ridge plateau rising to selected depths below the surface. The receiver was located 100 nm beyond the far side of the Ridge base (see Figure 6a). All propagation events used here assumed a flat pressure release surface and bottom characteristics as follows: sediment sound speed gradient of 0.1 m along the entire track; 0.2 dB/nm attenuation in the sediment from the source to the Ridge and a fully reflecting bottom at the Ridge and beyond. While this characterization is not realistic, runs performed using a highly absorbing bottom along the entire track differed in transmission loss versus depth characterizations by less than 3 dB overall with near bottom exponential roll-off starting at about 100 m shallower depth. The sound speed was assumed to be range dependent with the profile at the receiving site chosen to be that measured during the exercise and all others chosen from archival data for midsummer in the direction from the receiver to the southeast.

Figure 8 displays transmission loss versus depth profiles averaged over the 500 to 600 nm source-to-receiver range interval. Examining the depth dependence for such a range averaged transmission loss is equivalent to examining the noise field depth dependence for a uniform distribution of noise sources over the 500 to 600 nm range interval. The family of curves shown was obtained by repeating the simulation for a variety of Ridge crest depths (shown in the circle by each curve). Also shown on Figure 8 is the range averaged transmission loss depth profile resulting from a simulation with a single bottom depth (3300 m) and a single sound speed profile (that measured at Site 1 during the acoustic measurements). The first thing to note from Figure 8 is the significant increase in the portion of the water column depth with essentially constant average transmission loss which results from range dependent simulations (for the case of no bathymetric intrusion) as opposed to those from constant environment simulations. Thus, in the absence of the Reykjanes Ridge, one might anticipate a noise field of very nearly constant level with depth down to depths on the order of 3 km. As one would anticipate, the attenuation of energy carried by higher order modes resulting from the bathymetric intrusion by the Ridge results in confinement of the noise energy to shallower portions of the sound channel. Indeed, as the top of the (simulated) intrusion becomes shallower, the resulting distribution of energy (Figure 8) more and more nearly represents a single low order mode of the sound channel at the receiver site. Although none of the profiles of average transmission loss with depth in Figure 8 exactly matches the Site 1 data, the profiles do make the case that the bathymetric intrusion represented by the Ridge will significantly change the depth distribution of energy for noise sources across the Ridge from the receiver. Specifically, the Ridge combined with the local sound speed profile variation will tend to confine more energy to the upper portion of the water column. This tendency, the varying depth of the Ridge along its path between sources and receiving site, and contributions from sources not blocked by the Ridge (including at least a few at shorter range) conspire to produce the observed noise level versus depth profile.

AMBIENT NOISE BOUNDARY EFFECTS NEAR THE SEA SURFACE

During Dive 1 (Figure 2) AUTOBUOY made a slow ascent from approximately 360 m to 20 m below the surface (as indicated by its depth gauge signal) where it hovered for several minutes until it received the command to surface. During this ascent, as AUTOBUOY neared the surface, a radical change in the ambient noise level at low frequency was observed (see Figure 9). The level change during the last 340 m of depth change ranged from 11.5 dB at 25 Hz to 0.5 dB at 200 Hz for the upper hydrophone and from 7 dB at 25 Hz to 0.5 dB at 125 Hz for the deeper hydrophone. These two hydrophones, as mentioned earlier, are approximately 10 m apart so that when the upper hydrophone is at 20 m, the lower hydrophone is at 30 m depth. Assuming a directional noise field, these observations can be interpreted as a manifestation of the Lloyd Mirror Effect which basically states that the resultant output of a hydrophone near a boundary can be described as the algebraic sum of the output of the hydrophone and its image (the reflection of the hydrophone in the boundary taking into account the change in acoustic impedance at the boundary). For the case of a pressure release interface, the boundary effect results in a 180° phase change of the acoustic signal when reflected from the surface. Figure 10 displays effective vertical dipole beam patterns for a receiver at 20 m below the surface for two different frequencies; viz., 31 and 100 Hz. If the receiver were 60 m below the surface, then the 31 Hz pattern would be nearly identical to the 100 Hz pattern for a depth of 20 m. If the noise field were isotropic, integration over these two patterns for a single frequency but different receiver depths (say for 31 Hz at 20 and 60 m) would yield approximately the same value and therefore no significant depth effect would be noted. However, if noise is vertically directional as would be expected if the dominant sources are distant ships, then a significant decrease can be expected as the receiver approaches a boundary. Furthermore, the shape of the receiver dipole pattern is not changed for the horizontal null if the noise is band limited rather than single frequency. Note, in Figure 10, that the dashed curve for 1/3-octave noise is identical to that for a single frequency at the band center for the horizontal null and becomes progressively modified for subsequent nulls.

ANALYSIS OF NEAR SURFACE NOISE DEPTH DEPENDENCE

The pattern function for the dipole receiver, described above, is given by:

$$I = 4I_0 \sin^2\left(2\pi \frac{d}{\lambda} \sin \theta\right)$$

where the symbols are defined in Figure 11. The FANM noise model computes the noise energy arriving at a receiver in several vertical arrival angle bins. A special version of FANM was generated to apply the above pattern function separately to each vertical arrival angle bin (using the angle with the horizontal of the center of the bin as θ) and then sum the

resulting energy in the bins for a total (omnidirectional) noise level. This FANM version, producing what is called a coherent sum, was used to simulate the noise versus depth profiles for the upper hydrophone data of Figure 9. In these simulations, sharp decreases in level occurred at low frequency as the surface was approached. This is in contrast to a normal (incoherent) FANM calculation for which noise level either remains constant or actually increases slightly as a function of decreasing depth near the sea surface. In Figure 12, calculations with the new (coherent) FANM model are compared with the NORLANT '72 near surface data. The depth dependence of the data and the FANM simulations is in excellent agreement.

Recall that the FANM model cuts off noise energy which is blocked by bathymetric features. In the earlier discussion of the noise depth profile, it was postulated that the noise field at Site 1 resulted from a combination of noise energy, much of which had undergone varying degrees of bathymetric blockage by the Reykjanes Ridge. This was based in part on the information shown in Figure 8. In addition to a redistribution of energy in the deep portions of the water column, the bathymetric blockage modifies the near surface interference pattern. Figure 13 shows an expanded display of the near surface portion of the parametric, PE transmission loss study of Figure 8. Modification of the details of the near surface interference pattern by the bathymetric feature is evident. One persistent feature of the near surface interference pattern is the final monotonic decrease in noise energy as the receiver approaches the surface. This is a result of the pressure release surface and resulting exponential decay of all modes near the surface[12]. Reduction of the interference with increasing Ridge height (decreasing N) is consistent with the earlier description of higher order mode attenuation as the height of the bathymetric intrusion increases. Increased dominance of lower order modes can be interpreted as a reduction of ray angle, with the horizontal, for the interfering energy. From the equation of Figure 11, as the height of the bathymetric intrusion increases, the attendant decrease of should result in a shift to greater depth of various features of the interference pattern, such as the depth of occurrence of peaks and nulls. Just this behavior is exhibited by the results shown in Figure 13. For example, the first minimum in transmission loss (maximum of noise energy) occurs at its shallowest depth with no bathymetric interference and monotonically increases in depth as the Ridge height increases. The near surface features of the NORLANT '72 data are consistent with an interpretation of the field as a result of noise energy which has undergone varying degrees of bathymetric blockage by the Reykjanes Ridge. Note that the depth of the second (and higher order) nulls in the patterns of Figure 13 would be filled in by the 1/3-octave processing of the NORLANT data, although the first, near surface null would be unaffected (recall Figure 10). This and the reduction of the interference null by sea surface roughness are probable explanations for the absence of second and higher order nulls in the measured surface noise field.

CONCLUSION

In the NORLANT '72 data, both the near surface interference pattern and the depth profile of the noise field for the deeper portion of the water column

have been shown to be consistent with a postulated description of the noise field as a combination of noise energy fields from distant sources which have experienced varying degrees of blockage by the Reykjanes Ridge. Numerically simulated range averaged transmission loss has been shown to be a useful tool for analyzing the depth dependence of ambient noise fields. Such simulations have illustrated the impact of bathymetric blockage on both the noise versus depth profile in the deep portion of the water column and on the near surface interference pattern. Although they exhibited reasonable success in simulating the noise depth profile in the simpler region of the NORLANT '72 Dive 2, neither the DANES nor the FANM model was successful in reproducing the noise depth profile of more complicated origin at the Dive 1 site.

REFERENCES

1. Morris, G.B., August 1978. "Depth Dependence of Albient Noise in the Northeastern Pacific Ocean," JASA 64(2), 581-590.

2. Martin, R.L., May 1978. "NORLANT 72 Exercise Summary Report (U)," LRAPP Report S78-022, Naval Ocean Research and Development Activity, NSTL, MS.(SECRET)

3. Osborne, K.R., 1979. "DANES - A Directional Ambient Noise Prediction Model for FLENUMOCEANCEN," Report for Naval Ocean Research and Development Activity, Ocean Data Systems, Inc., San Diego, CA.

4. Cavanagh, R.C., 1974. "Fast Ambient Noise Model I (FANM I)," Acoustic Environmental Support Detachment, Office of Naval Research, Washington, D.C.

5. Tappert, F.D., 1977. "The Parabolic Approximation Method," in Wave Propagation and Underwater Acoustics, J.B. Keller and J.S. Papadakis, Eds., Lecture Notes in Physics, 70, 224-287, Springer-Verlag, New York.

6. Gozzo, R.S. and R.L. Martin, June 1973. "Autobuoy: Present Capabilities and Planned Modifications," NUSC TR 4505, Naval Underwater Systems Center, New London, CN.

7. Wenz, G.M., December 1962. "Acoustic Ambient Noise in the Ocean: Spectra and Sources," JASA 34(12), 1936-1956.

8. Perrone, A.J., September 1969. "Deep-Ocean Ambient-Noise Spectra in the Northwest Atlantic," JASA 46(3), 762-770.

9. Wagstaff, R.A., July 1977. "An Ambient Noise Model for the Northeast Pacific Ocean Basin (U)," JUA 27(3), 525-540. (CONFIDENTIAL)

10. Talham, R.J., August 1964. "Ambient-Sea-Noise-Model," JASA 36(8), 1541-1544.

11. Anderson, A.L. and K.C. Focke, April 1978. "Model Sensitivity Studies: Ambient Noise Depth Dependence Related to Propagation Loss (U)," JUA 28(2), 219-228 (CONFIDENTIAL)

12. Pedersen, M.A., D.F. Gordon. and D. White, September 1975. "Low-Frequency Propagation Effects for Sources or Receivers Near the Ocean Surface," NUC TR 488, Naval Ocean Systems Center, San Diego, CA.

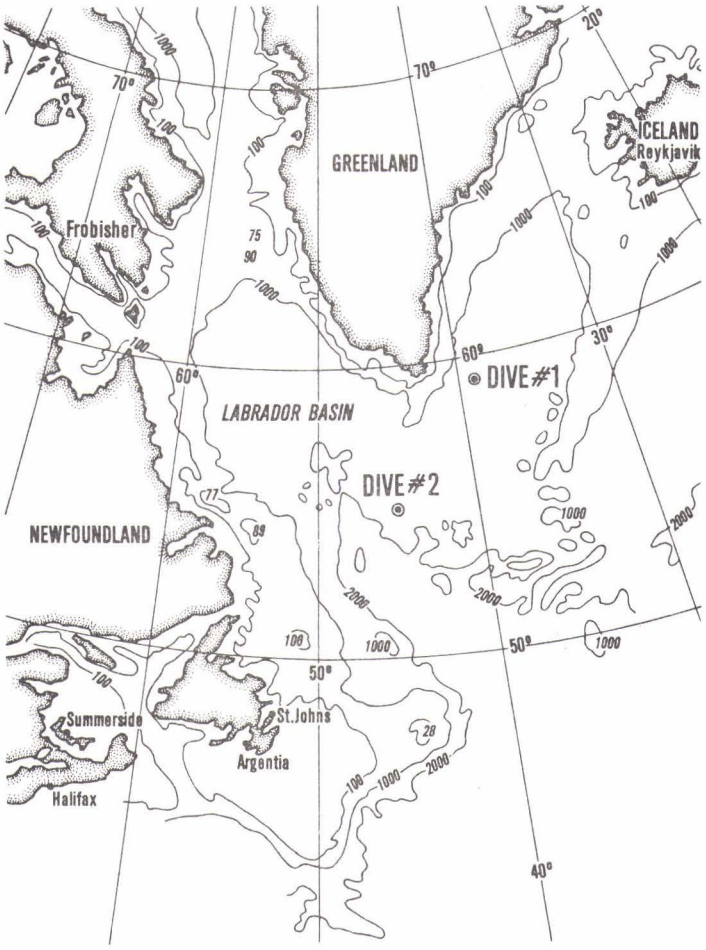

FIG. 1 LABRADOR SEA LOCATIONS

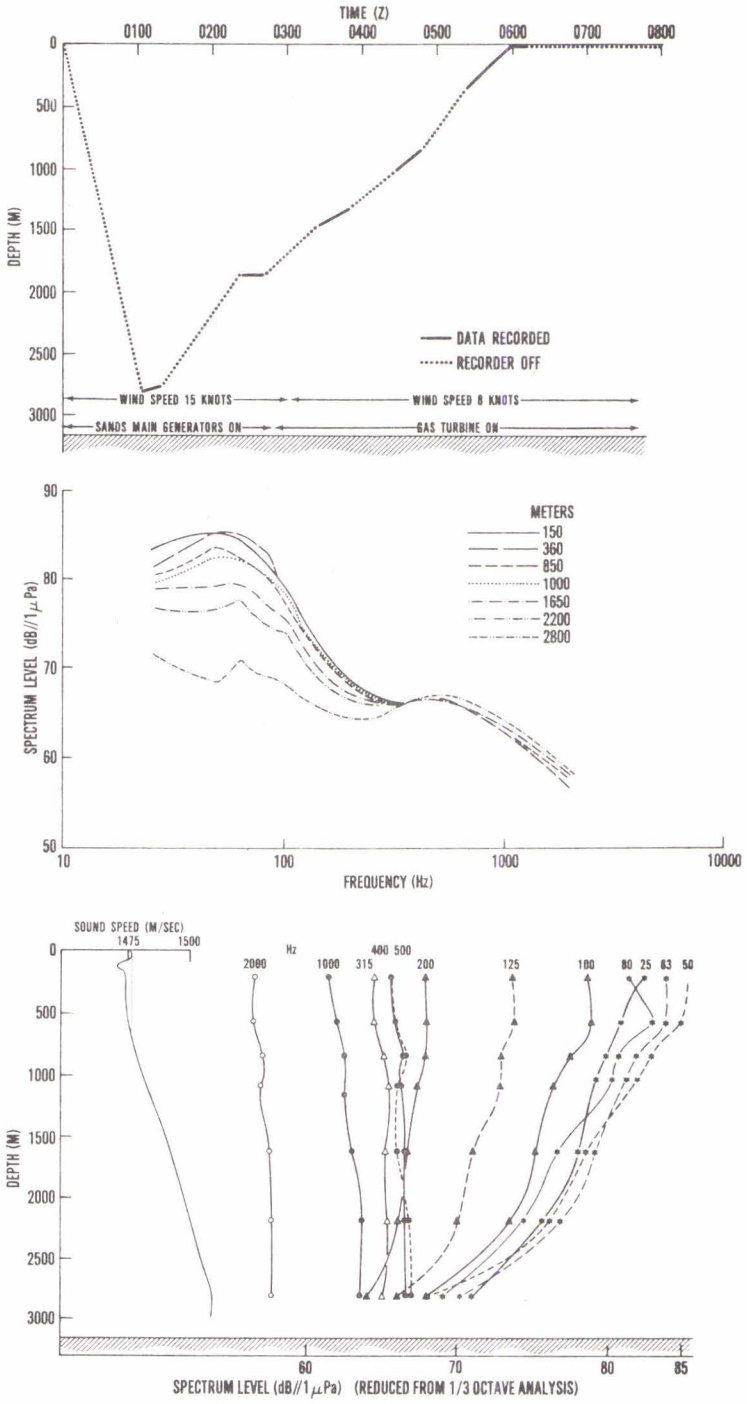

FIG. 2 DIVE 1: DIVE PATTERN; MEDIAN AMBIENT NOISE SPECTRUM; AMBIENT NOISE vs DEPTH

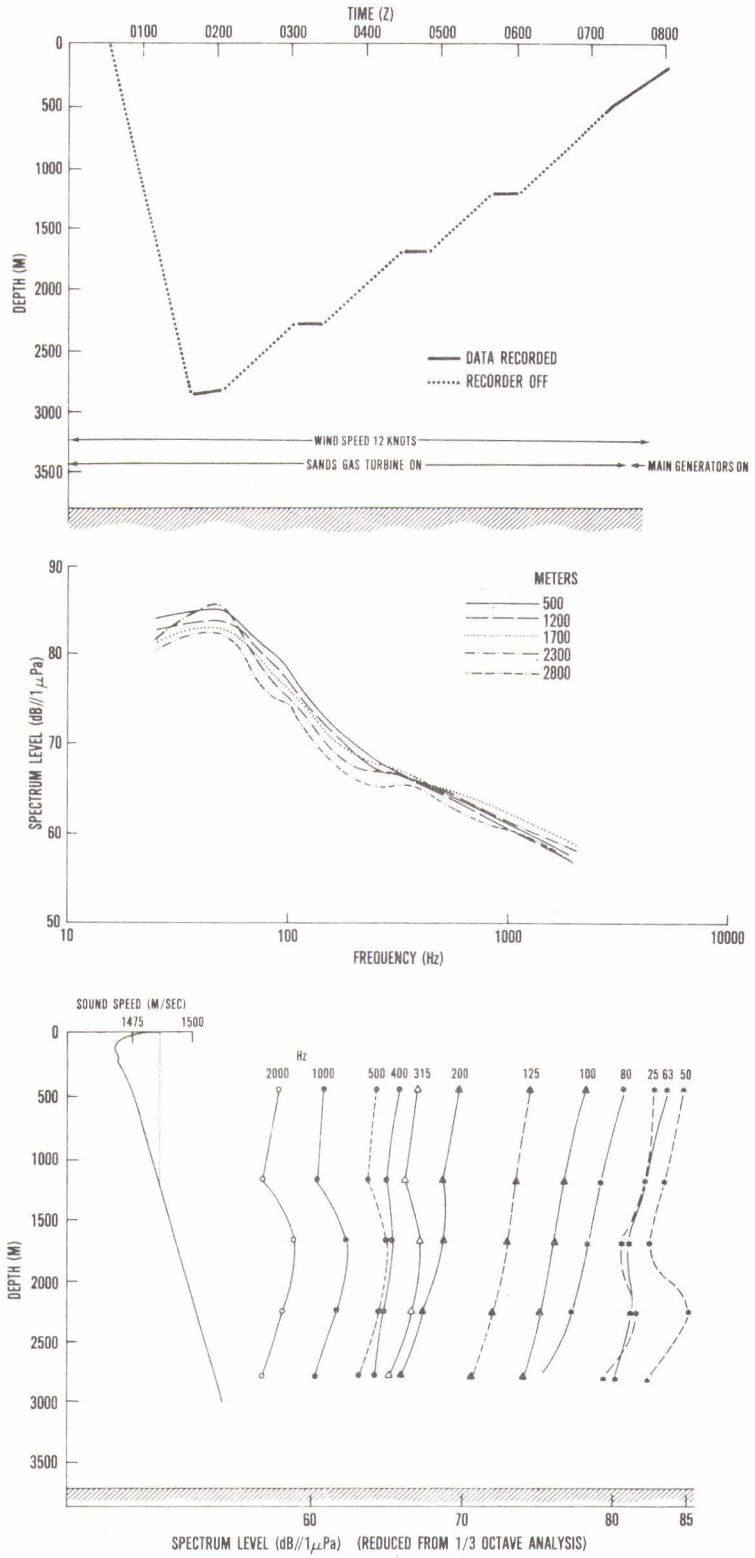

FIG. 3 DIVE 2: DIVE PATTERN; MEDIAN AMBIENT NOISE SPECTRUM; AMBIENT NOISE vs DEPTH

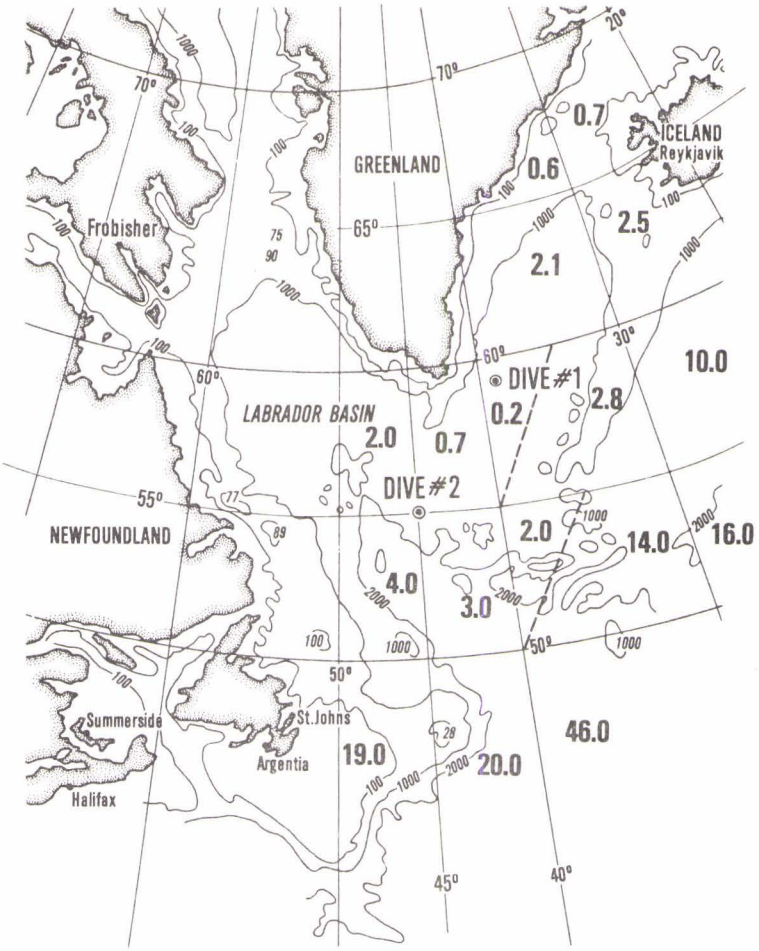

FIG. 4 SHIP COUNT, DAILY AVERAGE

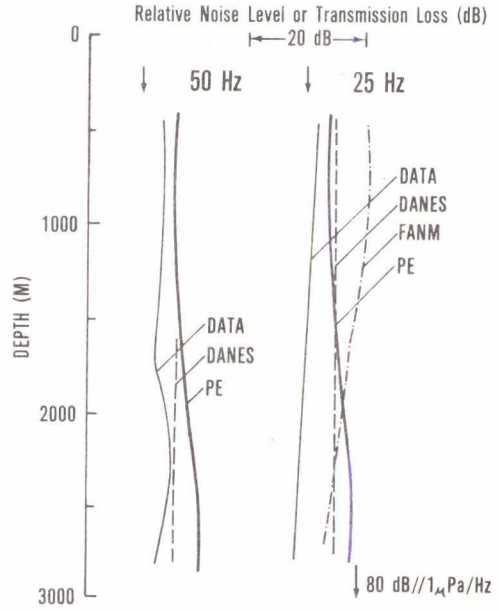

FIG. 5 DIVE 2: DATA MODEL COMPARISON

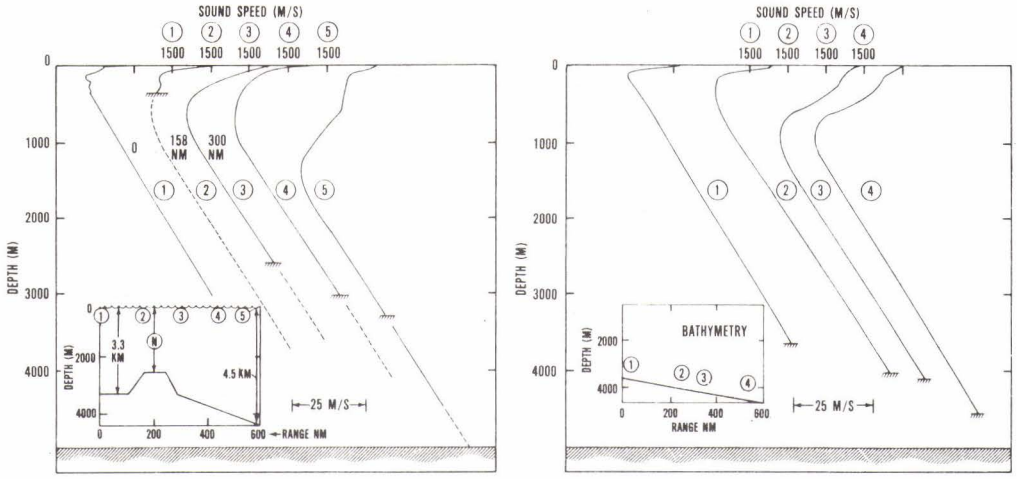

FIG. 6 ENVIRONMENTS FOR MODEL RUNS, DIVES 1 and 2

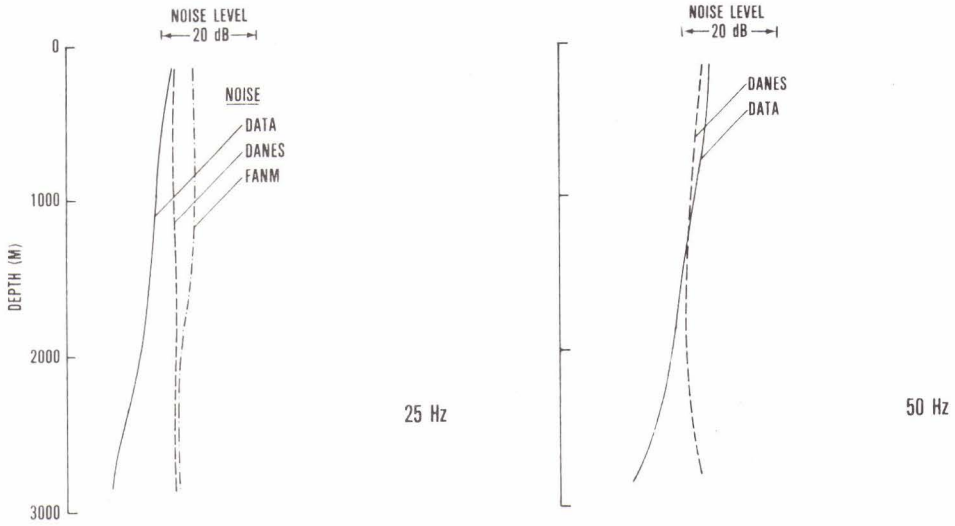

FIG. 7 DIVE 1: DATA MODEL COMPARISON

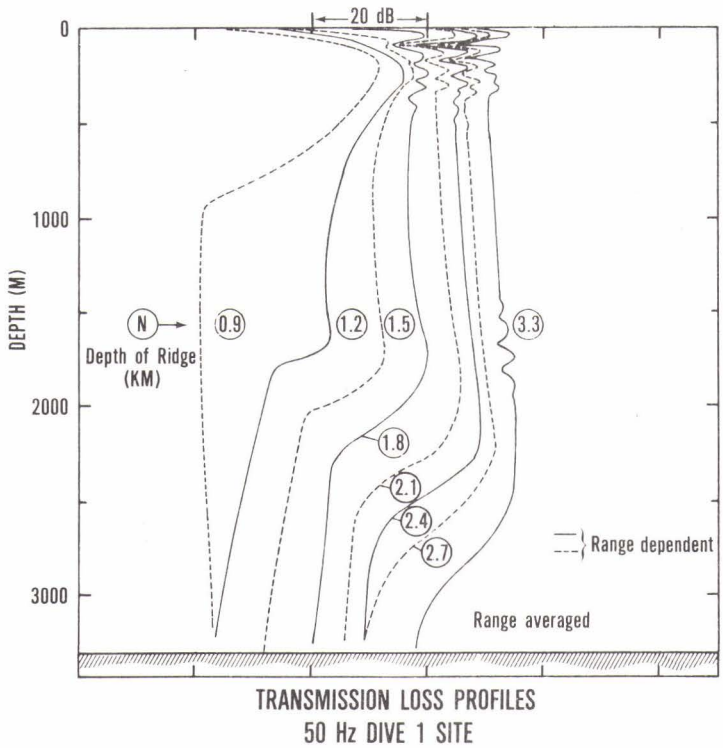

FIG. 8

DIVE 1: PARAMETRIC PE STUDY

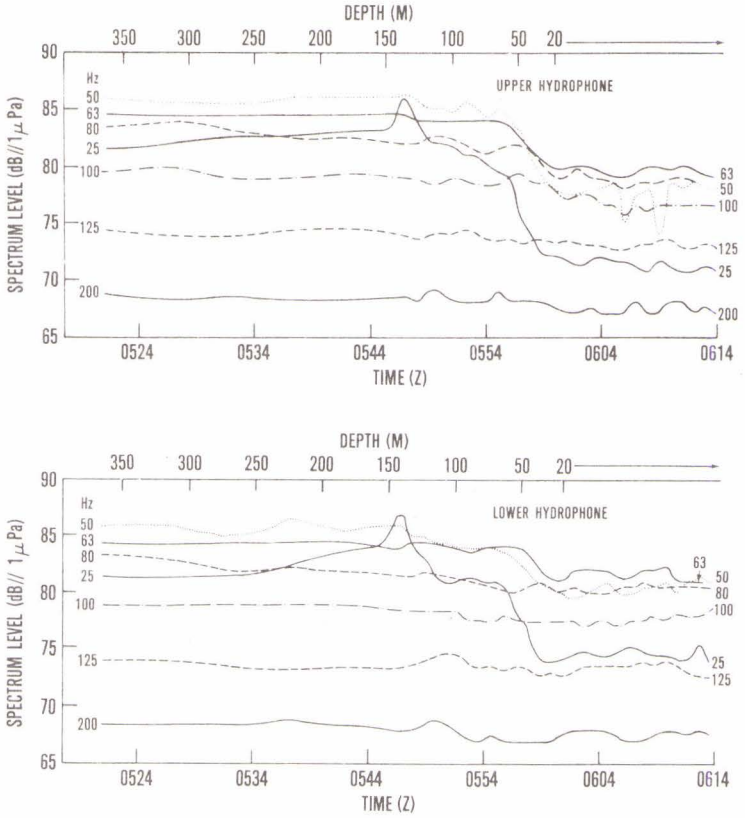

FIG. 9 DIVE 1: NEAR SURFACE AMBIENT NOISE DATA

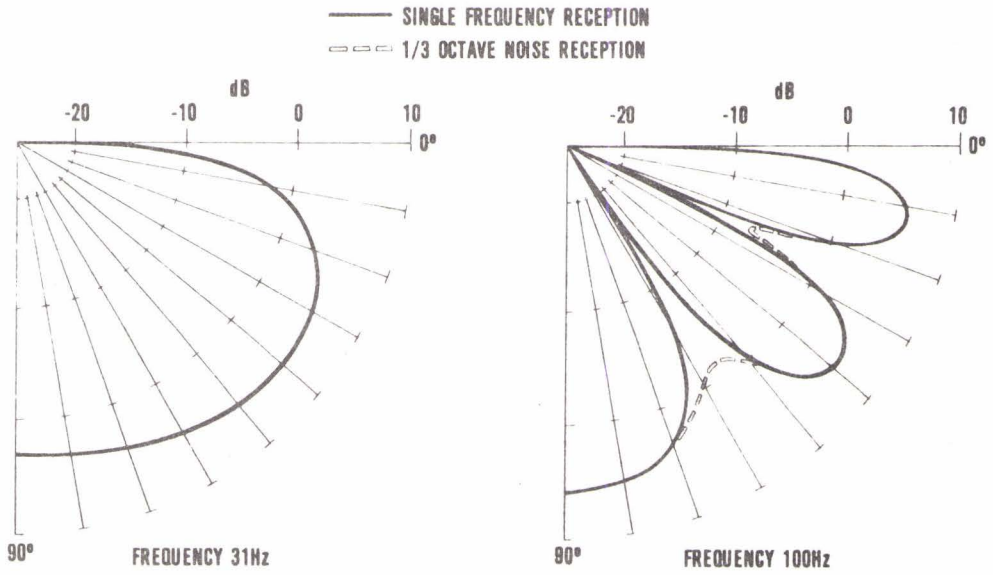

FIG. 10 VERTICAL DIPOLE BEAM PATTERN

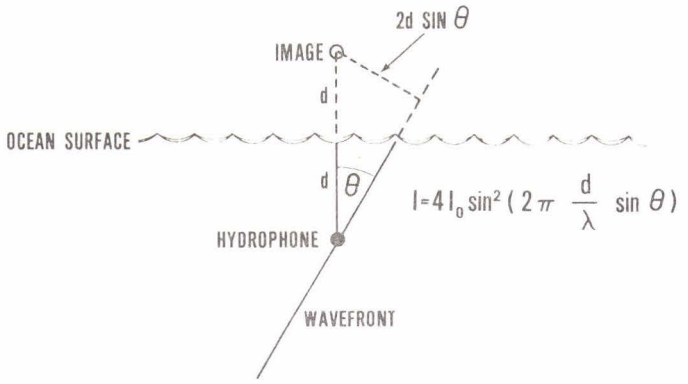

FIG. 11 GEOMETRY FOR VERTICAL DIPOLE BEAM PATTERN

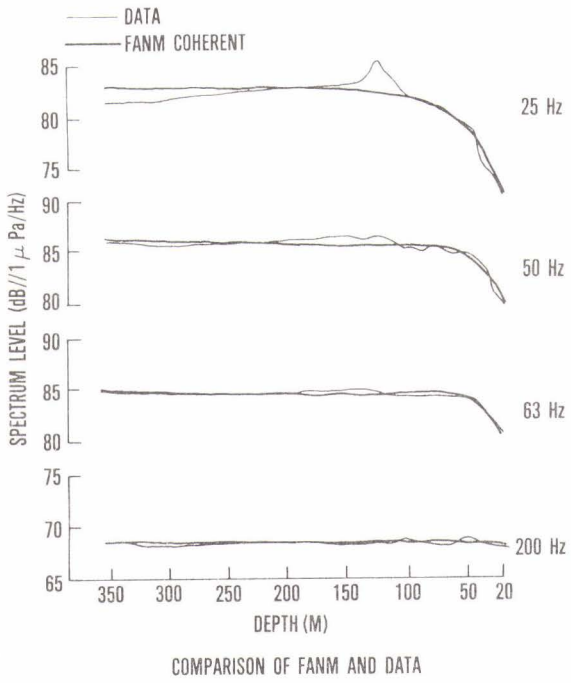

FIG. 12
DIVE 1:
NEAR SURFACE DATA MODEL COMPARISON

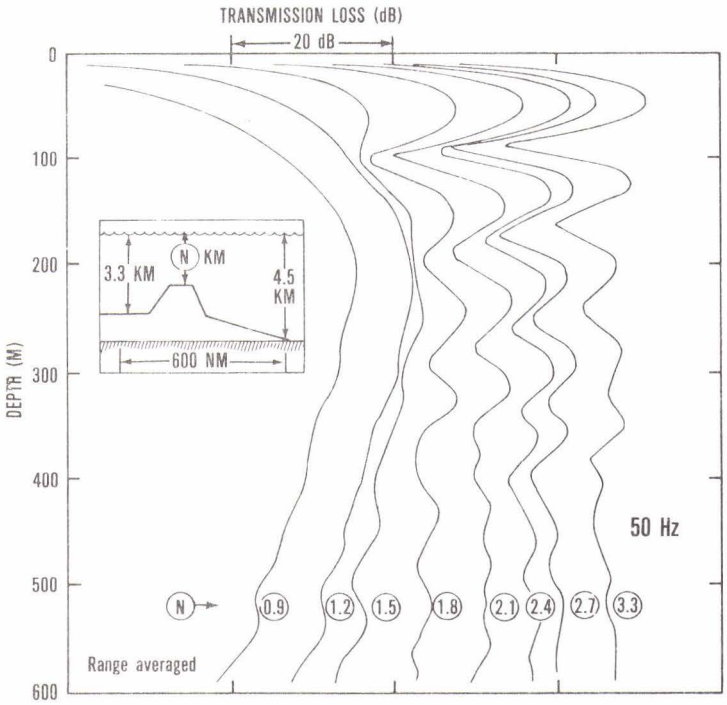

FIG. 13
DIVE 1:
NEAR SURFACE PARAMETRIC PE STUDY